environmental microbiology

Environmental Microbiology (2019) **00**(00), 00–00 doi:10.1111/1462-2920.14861

Pelagibacter metabolism of diatom-derived volatile organic compounds imposes an energetic tax on photosynthetic carbon fixation

Eric R. Moore, Cleo L. Davie-Martin,[†] Stephen J. Giovannoni and Kimberly H. Halsey*
Department of Microbiology, Oregon State University Corvallis, 354 Nash Hall, Corvallis, Oregon, 97331.

Summary

Volatile organic compounds (VOCs) produced by phytoplankton are molecules with high vapor pressures that can diffuse across cell membranes into the environment, where they become public goods. VOCs likely comprise a significant component of the marine dissolved organic carbon (DOC) pool utilized by microorganisms, but they are often overlooked as growth substrates because their diffusivity imposes analytical challenges. The roles of VOCs in the growth of the photoautotrophic diatom *Thalassiosira pseudonana* and heterotrophic bacterium *Pelagibacter* sp. HTCC1062 (SAR11) were examined using co-cultures and proton-transfer reaction time-of-flight mass spectrometry. VOCs at 82 *m/z* values were produced in the cultures, and the concentrations of 9 of these *m/z* values changed in co-culture relative to the diatom monoculture. Several of the *m/z* values were putatively identified, and their metabolism by HTCC1062 was confirmed by measuring ATP production. Diatom carbon fixation rates in co-culture with HTCC1062 were 20.3% higher than the diatom monoculture. Removal of VOCs from the *T. pseudonana* monoculture using a hydrocarbon trap caused a similar increase in carbon fixation (18.1%). These results show that a wide range of VOCs are cycled in the environment, and the flux of VOCs from phytoplankton to bacterioplankton imposes a large and unexpected tax on phytoplankton photosynthesis.

Received 17 July, 2019; revised 22 October, 2019; accepted 13 November, 2019. *For correspondence. E-mail halseyk@science.oregonstate.edu; Tel. (+541) 737 1831; Fax. 541-737-0496 [†]Present address: Terrestrial Ecology Section, Department of Biology, University of Copenhagen, Copenhagen Ø 2100, Denmark

Introduction

Photosynthetic diatoms and the heterotrophic bacteria *Pelagibacter* (SAR11) are both highly abundant in the surface ocean and make major contributions to biological carbon cycling. Microphytoplankton, a pigment-based classification primarily composed of diatoms, is estimated to carry out about 32% of net primary production in the ocean (Uitz *et al*., 2010). *Pelagibacter* are estimated to oxidize 6% to 37% of marine gross primary production (White *et al*., 2019). The flow of carbon between these two groups of organisms is therefore a potentially significant component of the marine carbon cycle.

Diatoms produce and release a wide variety of organic compounds that can vary depending on the species, growth status, and nutrient environment (Barofsky *et al*., 2009). Low-molecular-weight and volatile organic compounds (VOCs) have been associated with active growth (Colomb *et al*., 2008; Buchan *et al*., 2014), while more complex organic molecules are synthesized during senescence (Buchan *et al*., 2014). Production rates of both volatile and non-volatile organic compounds are dependent on light intensity (Halsey *et al*., 2017), nutrient availability (Bromke *et al*., 2013) and specific interactions with other microorganisms (Paul *et al*., 2012; Longnecker *et al*., 2015; Schmidt *et al*., 2015). VOCs are estimated to comprise 30%–40% of the dissolved organic carbon (DOC) pool that is the basis of the microbial food web (Dachs *et al*., 2005; Ruiz-Halpern *et al*., 2010; Hauser *et al*., 2013).

VOCs have a variety of roles in phytoplankton metabolism and ecology. VOCs can be important in signaling or grazing defense (Fink, 2007), support specific synergistic or antagonistic interactions with other microorganisms (Amin *et al*., 2015; Van Tol *et al*., 2016), provide protection from oxidative stress (Dani and Loreto, 2017), or are metabolic waste that may include products from overflow primary production (Schmidt *et al*., 2015; Srikanta Dani *et al*., 2017). In our study, we explore the possibility that some VOCs are intermediates or byproducts of metabolism that are uncontrollably lost from cells. Their low molecular weight, high vapor pressure, and, in many cases, hydrophobic properties enable VOCs to diffuse

across cell membranes (Bjørrisen, 1988; Shaw *et al*., 2003; Halsey *et al*., 2017). Uncontrollable losses of membrane-permeable organic compounds, including VOCs, could be promoted by heterotrophic removal of these compounds from the environment, and the loss of carbon by this mechanism is potentially taxing to primary producers (Bjørrisen, 1988).

Pelagibacter (*Pelagibacterales*) are ubiquitous, free-living heterotrophic bacterioplankton that have been shown to metabolize many low molecular weight, labile organic compounds, including VOCs (Giovannoni, 2017). As a result of genomic streamlining, *Pelagibacter* have specific carbon and nutrient requirements (Tripp *et al*., 2008; Carini *et al*., 2012) and have evolved to transport and metabolize a variety of phytoplankton-derived low-molecular-weight carbon compounds, including VOCs, using a limited genetic repertoire (Giovannoni *et al*., 2005). For example, *Pelagibacter* metabolize a variety of methylated and volatile compounds, including methanol, dimethylsulfide (DMS), formaldehyde, acetaldehyde, methylamine and methylated arsenic species (Sun *et al*., 2011, 2016; Halsey *et al*., 2017; Giovannoni *et al*., 2019).

The full diversity and quantity of VOCs produced by phytoplankton are unknown, but the multiple roles of these compounds in ecology and atmospheric chemistry make understanding their sources and sinks an important goal in marine microbial ecology. Microbial food web research often relies on the high-temperature catalytic oxidation method to determine the DOC pool available for heterotrophic consumption. However, this method systematically underestimates the volatile components in DOC (Bisutti *et al*., 2004); therefore, quantitative measurements of bulk VOCs in the ocean or in culture are rare (Hauser *et al*., 2013). Attention has primarily been given to a handful of compounds, such as DMS, methanol and acetone, which are known to be biologically cycled and have impacts on the atmosphere and climate (Sinha *et al*., 2007; Beale *et al*., 2013; Dixon *et al*., 2013).

To understand the dynamics and impacts of VOC exchange in marine microbial food webs, the growth and physiology of the diatom *Thalassiosira pseudonana* (CCMP 1335) and free-living heterotrophic bacterium *Pelagibacter ubique* (HTCC1062) were studied in monoculture and co-culture. *Pelagibacter* strain HTCC1062 (ecotype 1a.1) used in these experiments was originally isolated from Oregon coastal waters and is common in temperate and polar regions where diatoms, including *T. pseudonana*, contribute significantly to primary production at some times of the year. Proton-transfer reaction time-of-flight mass spectrometry (PTR-TOF/MS) was used to detect VOCs that changed in concentration in the co-culture relative to the diatom monoculture, revealing a wide range of VOCs that are substrates for *Pelagibacter* metabolism. Diatom carbon fixation rates increased both in the presence of the heterotroph and when VOCs were removed from the co-culture with a hydrocarbon trap. These results indicate that VOCs are an important conduit of carbon transfer between diatoms and *Pelagibacter* cells, and that the expense of VOC loss from phytoplankton cells imposes a significant tax on the energetics of photosynthetic carbon fixation.

Experimental procedures

Culture growth

Axenic stock and experimental cultures of *T. pseudonana* CCMP 1335 and *P. ubique* HTCC1062 were maintained in f/2 + Si artificial seawater medium (Guillard and Ryther, 1962) with the following modifications to support growth of HTCC1062: 0.939 mM KCl, 0.802 mM NO_3^-, 1.0 mM NH_4Cl, 0.05 mM glycine, 0.01 mM methionine, 0.078 mM pyruvate, 0.84 μM pantothenate, 0.985 μM 4-amino-5-hydroxymethyl-2-methylpyrimidine (HMP), 0.3 μM thiamine, 0.002 μM biotin, 0.117 μM $FeCl_3{\cdot}6H_2O$, 0.009 μM $MnCl_2{\cdot}4H_2O$, 0.0008 μM $ZnSO_4{\cdot}7H_2O$, 0.0005 μM $CoCl_2{\cdot}6H_2O$, 0.0003 μM $Na_2MoO_4{\cdot}2H_2O$, 0.001 μM Na_2SeO_3 and 0.001 μM $NiCl_2{\cdot}6H_2O$ (Carini *et al*., 2012, 2014). Following autoclaving, the growth medium was bubbled with 0.1 μm filter-sterilized carbon dioxide and air for 8 and 16 h, respectively, prior to use. Cultures were grown in 250–500 ml polycarbonate flasks or bottles at 16°C, under 25 μmol photons m^{-2} s^{-1} on a 12 h light–dark cycle, with gentle shaking at 60 rpm. Starting concentrations were 2×10^3 cells ml^{-1} for *T. pseudonana* or 2×10^5 cells ml^{-1} for HTCC1062 to allow both organisms to reach stationary phase at approximately the same time when in co-culture. For all co-cultures, both organisms were added to the medium at the same time, with the exception of the experiment where HTCC1062 was grown in co-culture without pyruvate, glycine or methionine additions. In this case, exponentially growing cultures of *T. pseudonana* were allowed to grow for 72 h prior to inoculation of HTCC1062. Cell densities of *T. pseudonana* were monitored with a Coulter counter (Beckman Coulter; Brea, CA) while HTCC1062 cells were stained with Sybr Green I and counted using a Guava Technologies flow cytometer (Millipore; Billerica, MA). All experiments and measurements were conducted while the cells were in exponential growth phase and approximately 3–6 h into the daylight portion of the light cycle.

For VOC removal experiments, 50 ml *T. pseudonana* monocultures were grown at 18°C and 25 μmol photons m^{-2} s^{-1} on a 12 h light–dark cycle. These cultures were grown in a closed system that re-circulated headspace air at 15–20 ml min^{-1} using a peristaltic pump. The headspace was circulated through a Supelpure HC hydrocarbon trap (Millipore-Sigma; St. Louis, MO) that removed

VOCs in a loop that flowed back directly into the growth medium. Headspace air in the control cultures was re-circulated in the same manner, except the carbon trap was omitted, thereby ensuring concentrations of CO_2, O_2, and physical turbulence from bubbling did not vary between treatments. Growth media was pre-treated by recirculating headspace air in this system for one week prior to the addition of cells, and continued to run as the cultures grew. *T. pseudonana* growth was monitored daily and harvested for carbon fixation and chlorophyll measurements after growth for about 1 week.

Carbon fixation measurements

First, 4 μCi of ^{14}C-labeled sodium bicarbonate was added to 9 ml subsamples of *T. pseudonana* monoculture or co-culture that were collected during mid-to-late exponential phase of growth. Working in the near-dark, samples were split into two aliquots and incubated at 25 μmol photons m^{-2} s^{-1}, or in the dark, for 20 min before terminating carbon uptake by adding 500 μl 1 N HCl. Prior to incubation, 50 μl of the ^{14}C-spiked sample was combined with 50 μl phenethylamine and 900 μl additional growth medium for total activity measurements. After samples were allowed to vent for 24 h, 1 ml of aliquot was combined with 5 ml EcoScint liquid scintillation cocktail, then measured using a scintillation counter (Beckman-Coulter; Brea, CA). pH measurements of each culture were also taken as a proxy for CO_2 concentrations, with no significant differences measured between culture pairs (mean difference = 0.03, p = 0.67, paired t test; n = 6). Cell enumerations by Guava flow cytometry indicated no bacterial contamination. One monoculture and co-culture pair, or ±VOC trap culture pair, was assayed at a time. These experiments were repeated several times, on different days, at the same point in the light cycle, using independent pairs of cultures. For each iteration, the treatment condition ('co-culture' or 'VOC removed') was compared directly with the associated *T. pseudonana* monoculture measured at the same time.

Photophysiology

Chlorophyll-a was extracted from cells by collecting 5–10 ml of culture onto glass fiber filters, which were then immersed in 5 ml 90% acetone, and stored at −20°C for 24 h. Absorbance from 400 to 800 nm of both extracted chlorophyll and whole filtered cells (total absorbance) was measured with a spectrophotometer (Shimadzu; Kyoto, Japan). Chlorophyll concentration was calculated according to the methods of Ritchie (2006). Total cellular absorbance from 400 to 800 nm was measured immediately after filtration and calculated according to Mitchell and Kieper (1988). Samples for pigment analysis by high-performance liquid chromatography (HPLC) were collected by the same filtration method, sealed in foil and flash frozen in liquid nitrogen and stored at −80°C until analysis by the Oregon State University HPLC facility using a modified version of the HPLC method of Wright *et al*. (1991) as described by Bidigare *et al*. (2005). Filters were extracted in 100% acetone for 24 h, at 4°C. Extracts were processed in reverse phase on a 250 mm C18 column using a Waters separations module and photodiode detector array. *Empower* chromatography software was used for integration and pigment quantification. The instrument was calibrated using chlorophyll-a from *Anacystis nidulans* (Millipore-Sigma; St. Louis, MO), and mixed pigment standards were obtained from DHI (Hørsholm, Denmark). F_v/F_m, a measurement of photosynthetic efficiency, was performed by diluting 100 μl of culture into 3.5 ml of fresh growth medium, then acclimated under dim blue light at 5 μmol photons m^{-2} s^{-1} for 5 min followed by an additional minute under complete darkness. Cellular fluorescence was then measured using a custom built fast repetition-rate fluorometer (Kolber *et al*., 1998).

ATP assays

Two hundred millilitres of HTCC1062 cultures were harvested by centrifugation in late exponential growth phase. Cell pellets were washed and re-suspended three times in modified f/2 + Si medium lacking glycine, methionine and pyruvate to remove residual growth substrates. Washed cells were re-suspended to 15 ml in the same f/2 medium and incubated in the dark at 16°C overnight. Starved cells were enumerated by flow cytometry, and then split into a minimum of three replicate 500 μl cultures in 2 ml sterile cryovials for each condition being tested. Individual VOCs (1 μM each), pyruvate (1 μM, positive control) or water (negative control) were added to the cultures, sealed tightly and incubated in the dark for 4 h. Cellular ATP was measured by adding 20 μl cell suspension to 90 μl Promega Bac-Titer Glo reagent (Promega; Madison, WI). Luminescence was measured using a luminometer (Tecan; Männedorf, Switzerland), set to 10 ms settle time and 1000 ms integration time, following mixing the sample for 5 s and incubating for 4 min at room temperature. Luminescence signal was compared with an ATP standard curve to calculate cellular ATP concentrations.

Proton-transfer reaction time-of-flight mass spectrometry

PTR-TOF/MS (Ionicon Analytik; Innsbruck, Austria) was utilized to measure VOCs in *T. pseudonana* monoculture and co-culture. Four replicates of monoculture and co-culture were grown in vented flasks for about 2 weeks, then destructively sampled 4–6 h into the daylight portion

of the light cycle while both species were in exponential growth phase. *T. pseudonana* cell densities in monoculture and co-culture were equalized across replicate cultures by the addition of fresh growth medium, which was identical to the medium used as the 'blank' control (Table 1). Then, 100 ml of culture was added to a VOC stripping chamber maintained at 16°C and 25 μmol photons m^{-2} s^{-1}, and bubbled through a glass frit in the bottom of the chamber with breathing grade air at 50 ml min^{-1} for 5 min to strip VOCs from the growth medium, and repeated for each replicate. This apparatus is described in Halsey *et al*. (2017). Each culture, and a blank fresh growth medium control, was measured independently using the same stripping chamber to reduce any effects due to variation in chamber construction or bubble production. VOCs stripped from the culture into the headspace were measured directly by the PTR-TOF/MS via soft/non-fragmenting ionization with H_3O^+. A mass spectrum ranging from 30–240 a.m.u was acquired at 5 s intervals over the course of 5 min. Each peak in the mass spectrum represents a compound of its molar mass + 1.008 (from the hydrogen ion). Because the first 2.5 min of the measurement was used to expel headspace from the chamber, only the last 2.5 min of data containing VOCs displaced from the culture medium were used in the analysis.

PTR-TOF/MS data were processed using the program *PTR-Viewer* (version 3.2.8.0) (Ionicon Analytik). Files were mass calibrated to three chemicals known to be present within each mass spectrum (*m/z* 29.998, 203.943, and 330.848). Initially, a mass binning approach was used to bin data at intervals of 0.5 mass units, bounded at 0.25 and 0.75 mass units (e.g. the *m/z* 59 bin ranged from 58.75 to 60.25). The precision of PTR-ToF/MS allows for the detection of small variations in mass, and as a result, some 0.5 mass unit bins contained multiple peaks generated by different compounds. The mass spectra were visually examined for multiple peaks within the same mass bin. All instances for which multiple peaks were identified were subsequently analyzed using a Gaussian-based approach to examine each peak individually. Integrated signals for each peak were normalized to primary ion (H_3O^+) concentrations, and concentrations for each mass peak were calculated. Only *m/z* values that had concentrations in culture greater than two standard deviations (SDs) above the blank growth medium concentration were considered in the downstream analysis. Mean concentrations of VOCs derived from monoculture and co-culture were then compared using a student's *t* test with a *p*-value significance cut-off of 0.05 ($n = 4$). Since a *t* test was performed for 82 different *m/z* values that had concentrations greater than the blank, resulting *p*-values were corrected for multiple hypothesis testing. The Benjimani–Hochberg procedure was applied with a *Q*-value cut-off ≤0.1 to reduce the likelihood of false positives.

Results

Culture growth

In growth medium replete with its known required organic carbon and reduced sulfur sources (pyruvate, glycine and methionine; Tripp *et al*., 2008; Carini *et al*., 2012), HTCC1062 had a generation time of 45.2 ± 0.9 h in co-culture with *T. pseudonana* and grew faster than the HTCC1062 monoculture (51.1 ± 1.3 h; $p = 1.7 \times 10^{-4}$, $n = 5$). Both cultures continued growing in exponential phase until nearly 1×10^8 cells ml^{-1}. There was no difference in generation times of *T. pseudonana* grown in monoculture and co-culture (42.0 ± 1.5 and 41.6 ± 1.2, $p = 0.63$, $n = 5$) (Fig. 1A and B). The faster growth rate of HTCC1062 in co-culture prompted us to ask if the diatom could support HTCC1062 growth even when its required growth substrates were not added to the medium. In co-culture with no added pyruvate, glycine or methionine, HTCC1062 attained a maximum cell density that was fourfold higher (7.9×10^6 cells ml^{-1}) than the HTCC1062 monoculture grown in the absence of pyruvate, glycine and methionine (1.2×10^6 cells ml^{-1}) (Fig. 1C). After 528 h, the HTCC1062 cell density in co-culture crashed contemporaneously with *T. pseudonana* reaching stationary phase (data not shown).

Production and consumption of VOCs in co-culture

We hypothesized that *T. pseudonana* produces VOCs that can be used as growth substrates by HTCC1062. PTR-TOF/MS was used to measure VOCs that had accumulated in the culture medium of *T. pseudonana* grown in monoculture and in co-culture with HTCC1062 after about 2 weeks of growth. In the monoculture and co-culture, 82 of 238 detected *m/z* values had concentrations greater than that of the fresh growth medium blank, and these *m/z* values ranged from 33.035 to 231.140 (Table 1). Of these 82 *m/z* values, 50 *m/z* values had higher concentrations than the blank in both the co-culture and *T. pseudonana* monoculture. Sixteen additional *m/z* values had concentrations that were higher in the *T. pseudonana* monoculture, but not the co-culture when compared with the blank, while 16 others were higher in the co-culture, but not in the *T. pseudonana* monoculture when compared with the blank (Table 1).

Nine *m/z* values were identified that significantly changed in concentration between the *T. pseudonana* monoculture and co-culture (Fig. 2A and B). Eight of the nine *m/z* values were lower in concentration in the co-culture compared with the *T. pseudonana* monoculture, with *m/z* 101.096 showing the largest relative decrease in co-culture concentration with a $\log_2$ fold-change of −1.24 (Fig. 2B). Several *m/z* values that changed in concentration in the co-culture compared with the *T. pseudonana* monoculture were putatively identified in Table 2 on the basis of their mass number and

Table 1. VOCs at 82 different *m/z* values were produced in the *T. pseudonana* monoculture and co-culture.

m/z	Blank conc. (ppbv)	TP conc. (ppbv)	TP SD	CC conc. (ppbv)	CC SD	*Q*-value	Culture
33.035	16.800	17.878	0.171	17.743	0.199	0.884	B
36.045	1.611	1.667	0.019	1.634	0.009	0.220	B
38.040	12.856	13.426	0.027	13.332	0.072	0.308	B
41.033	1.621	4.764	0.890	3.682	0.865	0.496	B
42.034	**1.821**	**2.790**	**0.107**	**2.491**	**0.112**	**0.092**	**B**
43.021	3.933	8.585	1.191	8.421	0.957	1.027	B
43.051	**1.775**	**5.029**	**0.392**	**3.609**	**0.429**	**0.039**	**B**
45.033	**11.463**	**17.510**	**2.300**	**8.930**	**2.542**	**0.041**	**T**
49.011	**3.600**	**4.905**	**0.836**	**10.591**	**1.463**	**0.032**	**C**
54.001	0.428	0.460	0.015	0.453	0.016	1.099	T
56.058	0.253	0.317	0.027	0.289	0.019	0.529	T
59.049	**8.863**	**20.874**	**1.372**	**16.700**	**1.482**	**0.076**	**B**
60.054	1.050	1.857	0.090	1.702	0.078	0.239	B
60.040	2.559	6.259	0.978	6.328	0.655	1.027	B
62.035	0.652	0.792	0.039	0.788	0.027	1.013	B
63.026	*0.866*	*1.513*	*0.117*	*1.256*	*0.052*	*0.145*	*B*
65.075	0.439	0.496	0.025	0.483	0.029	1.101	T
67.055	0.422	0.480	0.028	0.457	0.022	0.760	T
69.070	*0.920*	*1.550*	*0.144*	*1.218*	*0.137*	*0.140*	*B*
71.061	0.439	0.846	0.126	0.837	0.192	1.025	B
72.052	0.222	0.443	0.131	0.478	0.127	1.059	C
73.053	3.075	4.478	0.400	4.214	0.416	0.968	B
74.058	0.620	0.756	0.039	0.705	0.028	0.357	B
81.067	0.228	0.299	0.028	0.283	0.024	1.005	B
82.958	**0.157**	**0.332**	**0.027**	**0.169**	**0.010**	**0.015**	**T**
83.082	0.380	0.724	0.091	0.559	0.085	0.233	B
84.084	0.141	0.298	0.072	0.301	0.062	0.993	B
84.940	**0.286**	**0.374**	**0.011**	**0.285**	**0.004**	**0.005**	**T**
85.066	0.265	0.620	0.106	0.585	0.110	1.080	B
86.062	0.147	0.234	0.039	0.249	0.048	1.167	B
87.080	**0.660**	**1.387**	**0.120**	**0.944**	**0.101**	**0.029**	**B**
89.047	0.180	0.256	0.030	0.255	0.036	1.009	B
96.011	0.375	0.554	0.051	0.575	0.037	1.119	B
98.030	0.291	0.331	0.012	0.354	0.051	0.994	T
100.048	0.239	0.346	0.063	0.367	0.059	1.160	C
100.946	0.145	0.165	0.004	0.156	0.001	0.166	B
101.096	**0.218**	**0.728**	**0.027**	**0.309**	**0.031**	**0.000**	**B**
111.005	0.201	0.351	0.047	0.342	0.054	1.066	B
113.093	0.098	0.317	0.087	0.323	0.095	1.037	B
119.967	0.236	0.243	0.005	0.249	0.003	0.315	C
121.083	0.207	0.251	0.021	0.297	0.069	0.790	T
m/z	Blank	TP mean	TP SD	CC mean	CC SD	*Q*-value	T, C or B
121.985	0.127	0.136	0.004	0.144	0.011	0.780	T
123.105	0.126	0.188	0.029	0.197	0.029	1.055	B
123.960	0.211	0.217	0.006	0.220	0.003	1.080	C
125.978	0.127	0.151	0.011	0.151	0.016	0.999	T
127.097	0.141	0.417	0.073	0.370	0.067	0.963	B
128.095	0.085	0.122	0.012	0.118	0.008	1.119	B
129.115	0.141	0.235	0.024	0.217	0.023	0.874	B
130.080	0.079	0.099	0.005	0.094	0.008	0.906	T
135.087	0.123	0.180	0.025	0.168	0.020	1.080	B
138.036	0.066	0.098	0.012	0.095	0.012	1.074	B
140.100	0.065	0.089	0.012	0.086	0.011	1.148	T
141.100	0.078	0.179	0.029	0.150	0.023	0.573	B
143.133	0.098	0.180	0.027	0.176	0.030	1.042	B
143.948	0.079	0.091	0.004	0.090	0.005	1.064	B
145.107	0.062	0.073	0.004	0.071	0.005	1.122	T
149.037	0.099	0.161	0.027	0.161	0.030	1.001	B
151.096	0.065	0.152	0.055	0.146	0.040	1.008	C
153.084	0.066	1.203	0.443	1.028	0.292	1.099	B
153.256	0.025	0.209	0.081	0.187	0.054	1.114	B
155.080	0.072	0.233	0.078	0.236	0.070	0.983	B
156.116	0.046	0.070	0.009	0.069	0.008	1.055	B
157.131	0.063	0.103	0.016	0.100	0.016	1.045	B
167.095	0.051	0.093	0.025	0.123	0.025	0.517	C

(Continues)

Table 1. Continued

m/z	Blank conc. (ppbv)	TP conc. (ppbv)	TP SD	CC conc. (ppbv)	CC SD	*Q*-value	Culture
169.127	0.052	0.131	0.041	0.126	0.031	1.024	C
171.133	0.048	0.071	0.009	0.074	0.011	1.097	B
177.122	0.045	0.068	0.015	0.072	0.013	1.077	C
183.152	0.039	0.245	0.089	0.127	0.038	0.314	B
184.159	0.035	0.064	0.014	0.045	0.005	0.314	T
185.149	0.041	0.086	0.013	0.066	0.010	0.275	B
191.128	0.041	0.067	0.020	0.068	0.013	1.020	C
195.163	0.037	0.098	0.032	0.080	0.021	0.945	C
197.140	0.107	1.077	0.271	0.702	0.171	0.321	B
198.100	0.047	0.186	0.043	0.134	0.026	0.377	B
199.153	0.035	0.121	0.037	0.116	0.043	0.993	T
210.144	0.036	0.094	0.025	0.098	0.026	1.031	B
205.951	0.052	0.082	0.021	0.088	0.018	1.063	C
207.032	0.038	0.049	0.009	0.049	0.005	0.998	C
209.145	0.035	0.168	0.064	0.155	0.042	1.080	B
210.145	0.032	0.071	0.023	0.075	0.019	1.056	C
220.191	0.040	0.234	0.160	0.252	0.102	1.021	C
231.140	0.026	0.028	0.004	0.032	0.002	0.527	C

Of 238 *m/z* values detected, 82 *m/z* values had mean concentrations greater than 2 SDs above the blank measurement made with fresh growth medium. Of these 82 *m/z* values identified, 50 had concentrations higher than the blank in both monoculture and co-culture (B), 16 additional *m/z* values had concentrations higher in the *T. pseudonana* monoculture only when compared with the blank (T), while 16 others were higher than the blank in the co-culture only (C) – refer to 'culture' column. *Q*-value shows the results of the Benjimani–Hochberg statistical test used to compare concentrations between the monoculture and co-culture. Rows in bold indicate a *Q*-value less than 0.1.

previous reports of biogenic production by phytoplankton (Cotsaris *et al*., 1995; Colomb *et al*., 2008; Jüttner *et al*., 2010; Dani and Loreto, 2017; Halsey *et al*., 2017). As a result, we identified cyclohexanol, hexanal, cyclopentanol, acetaldehyde, acetonitrile, and acetone as compounds that changed significantly ($Q \leq 0.1$) in concentration in the co-culture compared with the diatom monoculture (Fig. 2, Table 2). Dimethyl sulfide (*m/z* 63.026) and isoprene (*m/z* 69.070), two important VOCs in the marine environment, marginally changed in concentration between the monoculture and co-culture (Fig. 2, Table 2). VOCs at *m/z* 82.958 and 84.940 were also lower in concentration in the co-culture relative to the monoculture. These two *m/z* values may be halogenated organic compounds, such as carbonyl chlorofluoride (*m/z* 82.958) or dichloromethane (*m/z* 84.940), which are reportedly produced in large quantities

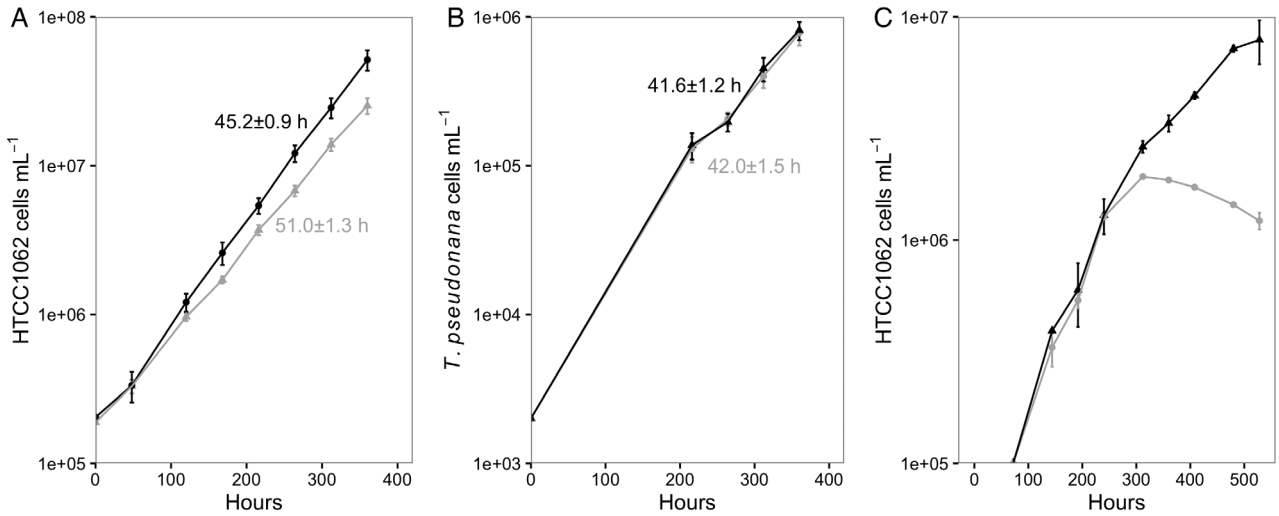

Fig. 1. HTCC1062 growth is enhanced by the presence of *Thalassiosira pseudonana*.
A. HTCC1062 generation times under carbon-replete conditions were nearly 6 h faster in co-culture (black) with the diatom compared with growth in monoculture (gray); $p = 1 \times 10^{-4}$, $n = 5$.
B. *T. pseudonana* growth rates were unchanged in the presence of the heterotroph (black = co-culture, gray = monoculture); $p = 0.67$, $n = 5$.
C. In medium lacking pyruvate, glycine and methionine, HTCC1062 was added to an exponentially growing *T. pseudonana* culture after 72 h (black) and reached a maximum density that was fourfold higher than the density reached by cells in monoculture also lacking pyruvate, glycine and methionine (gray) ($n = 3$). Error bars show SDs, *p*-values calculated using a student's *t* test.

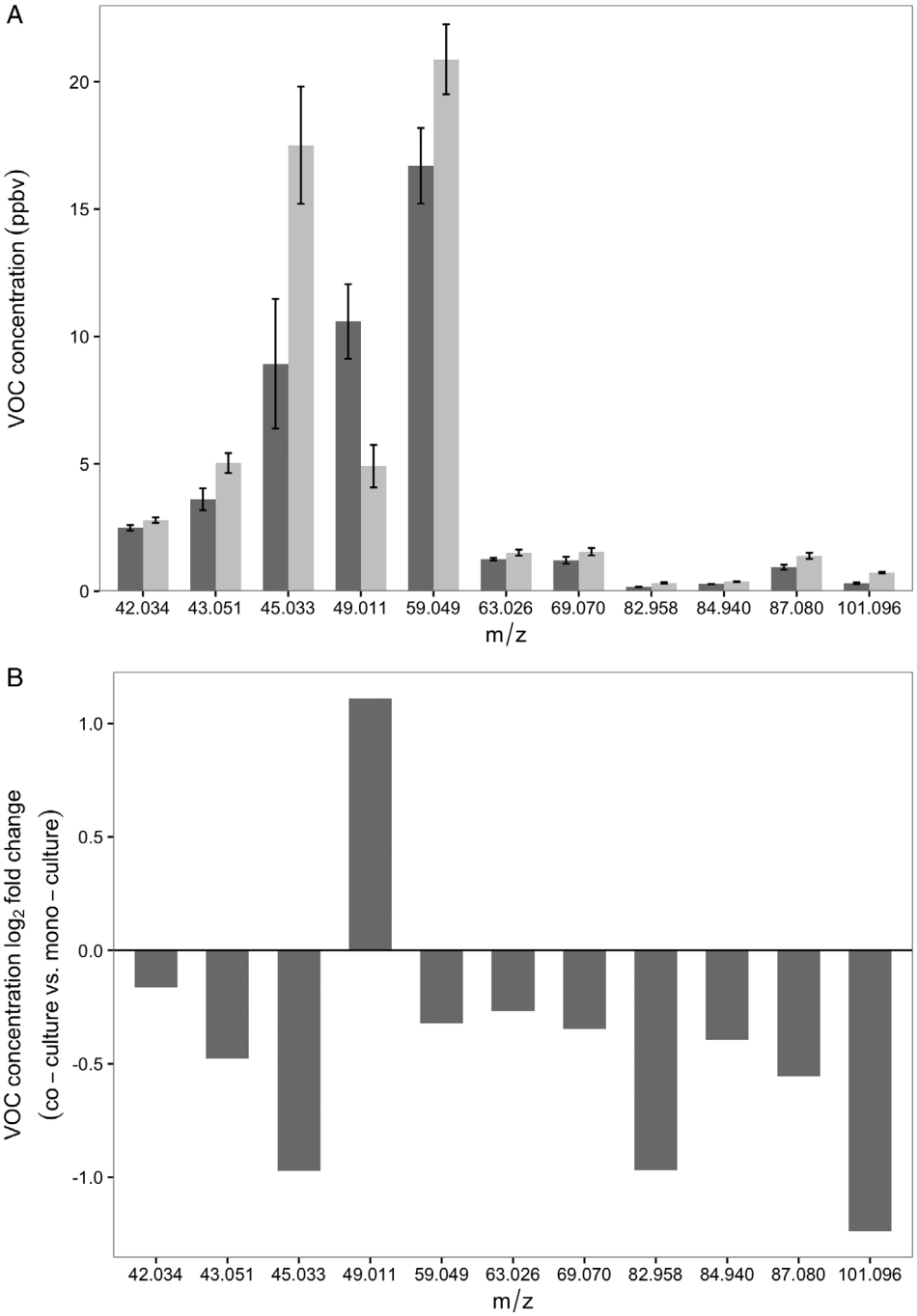

Fig. 2. HTCC1062 metabolizes a wide range of VOCs.
A. Concentrations of VOCs (shown along *x*-axis as *m*/*z*, equal to a compound's un-fragmented mass + 1) that differed in concentration in the *Thalassiosira pseudonana* HTCC1062 co-culture (dark bars) relative to the *T. pseudonana* monoculture (light bars); *T. pseudonana* cell densities were equal in all cultures.
B. Log_2 fold-change of VOC concentrations in the co-culture relative to the *T. pseudonana* monoculture for each *m*/*z* value. Putative identifications for each *m*/*z* are provided in Table 2.

by diatoms (Colomb *et al*., 2008; Paul and Pohnert, 2011). Halogenated compounds were not expected to be observed when running the PTR-TOF/MS in H_3O^+ mode, but ionization by contaminant O_2^+ ions originating from the ion source may have allowed for the detection of some halogenated compounds. One *m*/*z* value, 49.011 (methanethiol), was higher in concentration in the co-culture compared with the *T. pseudonana* monoculture, as might be anticipated since *Pelagibacter* have previously been identified as a methanethiol producer (Sun *et al*., 2016). There were no differences in the concentrations of compounds with *m*/*z* values larger than 101.096.

ATP measurements

A sensitive luciferase-based assay to measure cellular ATP was used to test whether HTCC1062 could metabolize the compounds we identified using PTR-TOF/MS. VOCs we putatively identified based on molecular mass and previous reports of production by phytoplankton (Cotsaris

Table 2. Putative identification of *m/z* values that differed in concentration in the co-culture relative to the *T. pseudonana* monoculture.

m/z	Putative VOC	Log_2 fold change in co-culture	*Q*-value
42.034	Acetonitrile	−0.163	0.08
43.051	*Propene*, *cyclopropane*	−0.479	0.04
45.033	Acetaldehyde	−0.971	0.03
49.011	Methanethiol	+1.110	0.03
59.049	Acetone	−0.322	0.06
63.026	DMS	−0.269	0.12
69.070	Isoprene	−0.348	0.12
82.958	*Carbonyl chlorofluoride*	−0.971	0.01
84.940	*Dichloromethane*	−0.393	0.004
87.080	Cyclopentanol, pentanal	−0.555	0.02
101.096	Cyclohexanol, hexanal	−1.237	<0.001

Chemical identifications made based on non-fragmented mass number, previous reports of the specific VOC being produced in phytoplankton, or metabolism by HTCC1062 determined by ATP assay (see Table 3). Compounds listed in italics are untested candidates for each respective *m/z* and provided on the basis of their molecular mass. The log_2 fold change (as in Fig. 2B) is the VOC concentration in co-culture relative to the VOC concentration in *T. pseudonana* monoculture. *Q*-value shows the results of the Benjimani–Hochberg statistical test used to compare concentrations between the monoculture and co-culture.

et al., 1995; Colomb *et al*., 2008; Jüttner *et al*., 2010; Dani and Loreto, 2017; Halsey *et al*., 2017) were fed to starved HTCC1062 cells. Acetone (*m/z* 59.049), isoprene (*m/z* 69.070) and two compounds representing *m/z* 101.096, hexanal and cyclohexanol, caused increases in cellular ATP content over the no-VOC-added control (Table 3). 2-Hexanone and *cis*-3-hexen-1-ol, which were also candidate compounds representing *m/z* 101.096, did not result in increases in cellular ATP content. Acetonitrile (*m/z* 42.034) concentrations changed between the monoculture and co-culture, and toluene appeared as a compound of interest early on in our analysis, but increased ATP content could not be confirmed in cells fed either of these compounds because of a large SD across replicates in this particular experiment. These data confirm that HTCC1062 can utilize a variety of VOCs as energy sources, thus the metabolism of these compounds by HTCC1062 may have resulted in their lower concentrations measured in the co-cultures. Since many different compounds with a wide variety of elemental compositions and structures can have the same mass number, we could not screen all of the chemical compounds that could represent each *m/z* value identified in Table 2. Consequentially, we cannot rule out that other VOCs sharing the same molecular mass contribute to the observed concentration changes in the PTR-TOF/MS *m/z* values.

Carbon fixation and photophysiology

Even though the presence of HTCC1062 did not cause a change in the growth rate of *T. pseudonana* when compared with its growth rate in monoculture (Fig. 1B), we considered the possibility that other photo-physiological changes may have been stimulated by HTCC1062. F_v/F_m experienced a slight drop from 0.62 in monoculture to 0.60 in co-culture, but there were no other evident differences in various measurements of diatom photo-physiology, including chlorophyll-a, total integrated cellular absorption, and measurements of other photo-pigment concentrations between the monoculture and co-culture (Table 4).

Photosynthetic carbon fixation was measured in seven independent pairs of *T. pseudonana* monoculture and co-culture. Carbon fixation varied between iterations of the experiment from 0.0249 to 0.0939 pmol C $cell^{-1}$ h^{-1}. Nevertheless, the average difference in carbon fixation between monoculture and co-culture pairs was 0.0139 pmol C $cell^{-1}$ h^{-1} (p = 0.05, paired t test, n = 7), equating to a mean increase of 20.3% in *T. pseudonana*

Table 3. VOCs were added to starved HTCC1062 (VOC added row) and cellular ATP content measured relative to negative controls (No VOC row).

	Isoprene[a]	Acetone[b]	Cyclohexanol[b]	Hexanal[c]	*Cis*-3-hexen-1-ol[c]	2-Hexanone[c]	Acetonitrile[d]	Toluene[d]
m/z	69.071	59.055	101.092	101.092	101.092	101.092	42.035	93.070
No VOC (− control)	2896 ± 247	3210 ± 172	3210 ± 172	3692 ± 108	3692 ± 108	3692 ± 108	4105 ± 2261	4105 ± 2261
VOC added	3318 ± 252	3631 ± 96	3845 ± 120	4185 ± 170	3739 ± 285	3501 ± 152	6167 ± 3114	6864 ± 1032
Pyruvate (+ control)	10,339 ± 1254	4533 ± 111	4533 ± 111	6629 ± 252	6629 ± 252	6629 ± 252	6707 ± 644	6707 ± 644
p-value	0.015	0.032	0.009	0.004	0.775	0.091	0.411	0.157

Increased cellular ATP content shows that the compound can be metabolized by HTCC1062 and supports our putative *m/z* value identification (Table 2). VOCs were supplied to HTCC1062 at 1 μM. Values are mean zeptograms ATP $cell^{-1}$ ± SD and *p*-values were calculated using a student's t-test vs. the negative control values for each experiment (isoprene n = 6, acetone and cyclohexanol n = 4, all others n = 3). Pyruvate was used as the positive control. Experiments testing different compounds were conducted with independent cultures on four different days (separated by vertical lines in table). Within a given experiment, all replicates and treatments were prepared with samples of the same culture. Due to variability between the days and reagent batches used, variability exists between the four experiments, thus comparisons should only be made to the controls for a given experiment.
Experiments with the same pyruvate or 'No VOC' values were conducted using the same HTCC1062 culture on the same day as indicated by columns with the same superscripted letters.

Table 4. Measurements of photo-physiological properties in *T. pseudonana* grown in monoculture or co-culture showed little detectable variation between conditions.

Parameter or pigment	*T. pseudonana* monoculture	Co-culture	Units	*p*-value
F_v/F_m	0.62 ± 0.00	0.61 ± 0.01	Unitless	0.05
Total absorbance	0.0116 ± 0.0012	0.0135 ± 0.0014	m^2 mg^{-1}	0.13
Chlorophyll a	0.7247 ± 0.0209	0.7541 ± 0.0617	pg $cell^{-1}$	0.50
19′-Hexanoyloxyfucoxanthin	0.0018 ± 0.0003	0.0016 ± 0.0005	pg $cell^{-1}$	0.64
β-Carotene	0.0219 ± 0.0012	0.0193 ± 0.0019	pg $cell^{-1}$	0.13
Chlorophyll b	0.0100 ± 0.0014	0.0099 ± 0.0009	pg $cell^{-1}$	0.95
Chlorophyll c	0.0758 ± 0.0117	0.0688 ± 0.0043	pg $cell^{-1}$	0.41
Chlorophyllide	0.0222 ± 0.0046	0.0293 ± 0.0043	pg $cell^{-1}$	0.12
Diadinoxanthin	0.0420 ± 0.0023	0.0394 ± 0.0039	pg $cell^{-1}$	0.37
Fucoxanthin	0.2737 ± 0.0105	0.2603 ± 0.0181	pg $cell^{-1}$	0.34
Lutein	0.0010 ± 0.0006	0.0012 ± 0.0003	pg $cell^{-1}$	0.51
Violaxanthin	0.0031 ± 0.0003	0.0027 ± 0.0002	pg $cell^{-1}$	0.16
Zeaxanthin	0.0015 ± 0.0008	0.0010 ± 0.0002	pg $cell^{-1}$	0.42
Total carotenes	0.0219 ± 0.0012	0.0193 ± 0.0019	pg $cell^{-1}$	0.13

Values are the average of three biological replicates ± SD.

carbon fixation in the co-culture compared with the monoculture (Fig. 3A). Accumulation of the ^{14}C tracer in bacterial biomass through inorganic carbon fixation was ruled out because the mean increase in carbon fixation by the diatoms in the co-cultures was 9.51×10^3 pmol C ml $culture^{-1}$ h^{-1}, but incorporation of the labeled inorganic carbon by HTCC1062 was only 1.07×10^1 pmol C ml $culture^{-1}$ h^{-1}, about three orders of magnitude less than the average difference in carbon fixation between the *T. pseudonana* monoculture and co-culture.

We hypothesized that the metabolism of VOCs by HTCC1062 stimulated the faster rate of carbon fixation in *T. pseudonana* in co-culture relative to the monoculture. To test this idea, we replaced the biological VOC sink (i.e. HTCC1062) with a physical VOC sink – a hydrocarbon trap in a circulating gas loop. When VOCs were

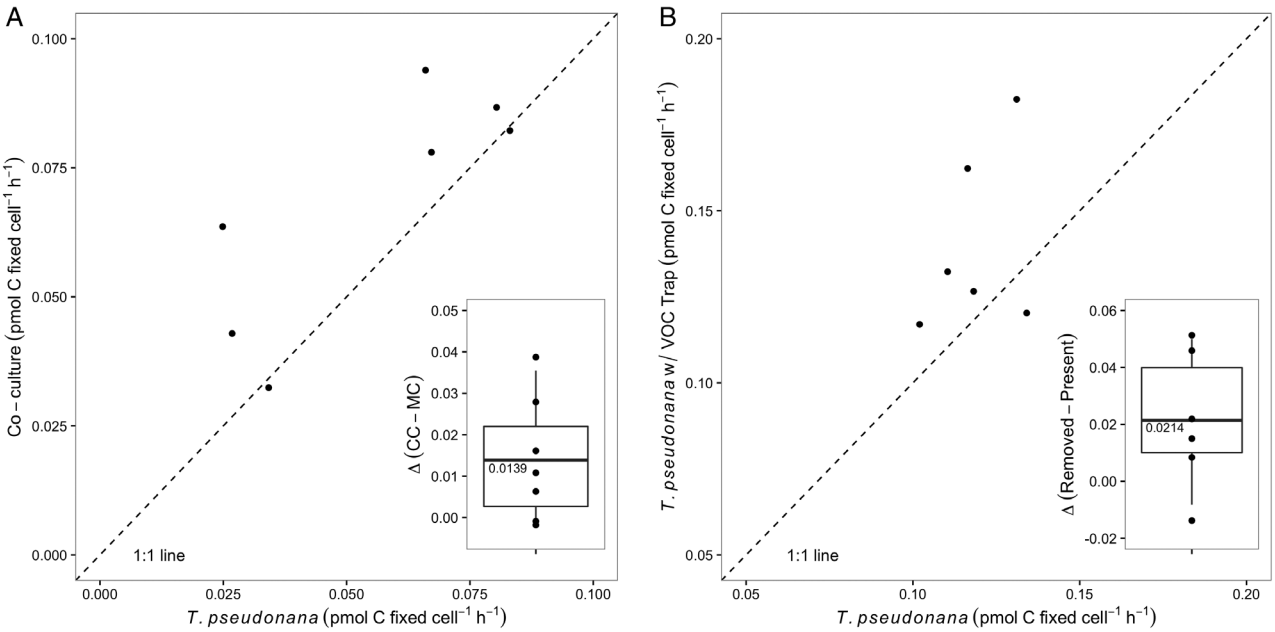

Fig. 3. VOC efflux causes an increase in photosynthetic carbon fixation in *Thalassiosira pseudonana*.
A. *T. pseudonana* carbon fixation increased an average of 0.0139 ± 0.0139 pmol C $cell^{-1}$ h^{-1}, [mean ± 95% confidence interval (CI), $p = 0.050$, paired *t* test, $n = 7$] in co-culture with HTCC1062 compared with *T. pseudonana* monocultures, a mean increase of 20.3%.
B. Physical removal of VOCs in *T. pseudonana* monocultures using a hydrocarbon trap increased carbon fixation by an average of 0.0214 ± 0.0255 pmol C $cell^{-1}$ h^{-1}, an 18.1% increase on average (mean ± 95% CI, $p = 0.083$, paired *t* test, $n = 6$).
Points in both A and B are measurements for independent pairs of monoculture and co-culture (A) or independent pairs of cultures with VOC-present and VOC-removed (B). Dashed line is the 1:1 relationship. Points falling above the 1:1 line indicate more carbon was fixed in co-culture or in the VOC-removed condition than in the monoculture or in the VOC-present control. Differences (Δ) between carbon fixation for each pair are shown in the subplots, where the box shows the mean (value given), and upper and lower quartile divisions; whiskers show 95% CI.

continuously removed from the *T. pseudonana* cultures using the hydrocarbon trap, carbon fixation increased by an average of 0.0214 pmol cell^{-1} h^{-1} (18.1%) compared with normal cultures containing VOCs (Fig. 3B, $p = 0.08$, paired *t* test, $n = 6$]. Similar to the growth experiments in the presence and absence of HTCC1062, *T. pseudonana* growth rates were unaffected by the presence or absence of VOCs (0.57 $\pm$ 0.02 and 0.56 $\pm$ 0.04 day^{-1} respectively).

Discussion

The total VOC pool has attracted attention as a potentially significant component of phytoplankton-derived DOC in the marine environment (Myklestad, 2000; Thornton, 2014), but the magnitude of VOC flux between phytoplankton and bacterioplankton and the suite of compounds involved have not been characterized with enough precision and detail to draw definitive conclusions. Two studies suggested that 30% to 40% of marine DOC is composed of VOCs (Dachs *et al*., 2005; Ruiz-Halpern *et al*., 2010), but methodological issues confounded those results (Hauser *et al*., 2013). There is also uncertainty about variation in the contributions of VOCs to the DOC pool across different ocean regions and time scales, which are needed to close the carbon budget and define the roles of VOCs in marine ecology and their impacts on atmospheric processes (O'Dowd and de Leeuw, 2007; Facchini *et al*., 2008; Spracklen *et al*., 2008).

We designed experiments with two taxa that are important carbon cycle contributors in productive temperate coastal ocean regions, and studied their VOC-associated interactions with analytical methods that were not confined to known targeted VOCs. VOCs known to be produced by diatoms, including acetone (*m/z* 59.049) and cyclohexanol (*m/z* 101.096) (Cotsaris *et al*., 1995; Colomb *et al*., 2008; Dani and Loreto, 2017; Halsey *et al*., 2017; Srikanta Dani *et al*., 2017), were identified and shown to be metabolized by the common heterotroph *Pelagibacter*, which co-occurs in diatom habitats. Unexpectedly, consumption of these VOCs by *Pelagibacter* imposed a significant energetic tax on *T. pseudonana* by decoupling photosynthetic carbon fixation from growth. To explain these observations, we postulate that some VOCs used by *Pelagibacter* are volatile metabolic intermediates in phytoplankton biochemical pathways that enter a pool of public goods. In this conceptual model, *Pelagibacter* metabolism of these public goods imposes an energetic tax by requiring the diatom to more rapidly fix carbon to maintain intracellular pools of volatile metabolites.

Growth of HTCC1062 in co-culture with *T. pseudonana* caused VOCs at nine different *m/z* values to change in concentration relative to *T. pseudonana* monocultures. Eight of these *m/z* values decreased in concentration in the co-culture, suggesting that the metabolism of VOCs by HTCC1062 resulted in their lower observed concentrations in co-culture. An alternative interpretation of these data is that, in the co-culture, the production of these VOCs by *T. pseudonana* was diminished by the presence of HTCC1062. The first explanation is more likely because when VOCs representing several *m/z* values were fed to HTCC1062 in monoculture, ATP content in the cells increased (Table 3). Additionally, we observed a decrease in the concentrations of *m/z* 45.033 (acetaldehyde) and 63.026 (DMS), as well as an increase in the concentration of *m/z* 49.011 (methanethiol), findings that are consistent with previous reports showing HTCC1062 metabolism of acetaldehyde and DMS, and formation of methanethiol as a waste product of dimethylsulfoniopropionate (DMSP) metabolism (Sun *et al*., 2016; Halsey *et al*., 2017). Thus, we can add acetone, isoprene, cyclohexanol and hexanal to the growing list of VOC substrates used by *Pelagibacter*, but the rates and mechanisms of their metabolism remain to be determined. Acetonitrile and toluene marginally increased in ATP content; however, significant variability in this particular experiment prevented us from confirming HTCC1062 metabolism of these compounds by this approach. Significant, yet modest increases in cellular ATP content when supplied the VOCs shown in Table 3 indicate that certain VOCs can be utilized by HTCC1062, but they do not provide as much ATP as pyruvate, a required growth substrate. However, the collective impact of many different VOCs utilized simultaneously by HTCC1062 in co-cultures or in the environment could additively constitute a significant energy input for cell metabolism.

Recent work examining bacterial metabolism of VOCs in the marine environment has shown that a limited but diverse array of marine heterotrophic bacterioplankton are able to harvest VOC compounds and use them to supply elemental quotas or energy (Sun *et al*., 2011; Halsey *et al*., 2012, 2017; Dixon *et al*., 2014; Johnston *et al*., 2017; Sargeant *et al*., 2018). For example, acetone metabolism rates in seawater were positively correlated with the abundance of low nucleic acid bacteria, which dominated the community and included *Rhodobacteriales* and SAR11/*Pelagibacter* (Dixon *et al*., 2014). Similarly, the abundance of SAR11 was correlated with rates of methanol oxidation and explained up to 59% of methanol oxidation in oligotrophic environments (Sargeant *et al*., 2018). *Rhodococcus*, *Gordonia* and *Mycobacterium* were enriched in seawater incubated with isoprene (Johnston *et al*., 2017), and the evolutionarily distant methylovore HTCC2181 (Betaproteobacteria) metabolized a variety of VOCs, including methyl chloride and methanol (Halsey *et al*., 2012). Aside from these few examples, the microbes responsible for metabolizing VOCs in the ocean and the biochemical pathways involved remain relatively unknown.

T. pseudonana supported the growth of *Pelagibacter* HTCC1062 with no added pyruvate, glycine or methionine (Fig. 1C), and enhanced HTCC1062 growth rates under carbon replete conditions in co-culture (Fig. 1A). These data show that *T. pseudonana* produced compounds that met the unusual requirements of HTCC1062 for reduced sulfur compounds, glycine or glycine precursors, and alanine or alanine precursors (Tripp *et al*., 2008; Carini *et al*., 2012, 2014). The ubiquitous cyanobacterium, *Prochlorococcus*, was also observed to support growth of a related *Pelagibacter* strain, HTCC7211, in co-culture. Similar to HTCC1062 growing with *T. pseudonana*, HTCC7211 exhibited enhanced growth during the *Prochlorococcus* exponential phase and a rapid decline in cell density when *Prochlorococcus* reached stationary phase (Becker *et al*., 2019), potentially due to a shift in the types of exometabolites produced as the phytoplankton reaches stationary phase (Barofsky *et al*., 2009; Longnecker *et al*., 2015). Exometabolite production, including VOCs, differs among phytoplankton (Halsey *et al*., 2017; Landa *et al*., 2017), but in the two examples of phytoplankton co-cultured with *Pelagibacter* reported so far, the phytoplankton exometabolites were sufficient to support growth when required growth substrates were omitted from the growth medium, with the exception of vitamins such as HMP, which were not tested in either study (Becker *et al*., 2019). The volatile components of DOC produced by *T. pseudonana* were demonstrated to be sources of energy for HTCC1062, as some of the identified VOCs stimulated ATP production by the bacteria, but their contribution to the observed growth enhancement of HTCC1062 in co-culture remains uncertain, with the exception of acetaldehyde (*m*/*z* 45.033), which can be incorporated into HTCC1062 biomass (Halsey *et al*., 2017). Experiments examining the metabolism of VOCs by HTCC1062 in greater detail are necessary to understand their importance as substrates, but studies on the metabolism of other carbon substrates by the SAR11 clade indicate that many organic compounds are oxidized for energy, rather than used for growth (Sun *et al*., 2011; Halsey *et al*., 2017; Giovannoni *et al*., 2019).

The propensity of low-molecular-weight, non-polar or hydrophobic volatile compounds to diffuse through the cell membrane (Bjørrisen, 1988) means that they can be uncontrollably lost from cells. For photoautotrophs, this carbon loss can be taxing to the energetics of their growth, especially in small cells with low surface area to volume ratios, unless a relatively high environmental concentration of VOCs exists to maintain equilibrium with the VOCs inside the cell (Bjørrisen, 1988). In principle, the consumption of VOCs by heterotrophic organisms would promote the flux of VOC metabolites from the phytoplankton cells into the environment. We found support for this interpretation in the observation that we could simulate continuous bacterial VOC consumption by recirculating the headspace air in *T. pseudonana* monocultures through a hydrocarbon trap. Removal of VOCs using this method caused an 18.1% increase in carbon fixation compared with cultures containing VOCs, without altering growth (Fig. 3B). Comparably, HTCC1062 caused *T. pseudonana* carbon fixation to increase by 20.3% in the co-culture (Fig. 3A). These results suggest that the removal of VOCs from the culture medium stimulated diffusional efflux of VOCs from *T. pseudonana*, and the cells responded to this loss of carbon by increasing carbon fixation. This response implies that phytoplankton depend on the availability of volatile compounds to maintain metabolic efficiency and constant growth rates. A similar phenomenon is shown to occur in bacterial cultures producing siderophore public goods under iron limitation, where siderophore production by *Pseudomonas aeruginosa* was higher in the presence of cheater cells that steal, but do not synthesize siderophores (Weigert and Kümmerli, 2017). Thus, VOCs are another example of a public good that can be exploited by the broader microbial community at the expense of the VOC producer.

Phytoplankton are sources of diverse VOC compounds, some of which have been identified as by-products or intermediates in biochemical pathways, such as carotenoid synthesis (Schmidt *et al*., 2015). Some VOCs are reported to function as antioxidants in higher plants and algae, and protect phytoplankton cells from reactive oxygen species, especially in high light conditions (Dani and Loreto, 2017). Although the roles of VOCs in metabolism are known in only a few cases, our findings are consistent with the interpretation that VOCs are metabolic intermediates and therefore the depletion of the VOC pool by physical or biological sinks requires cells to respond by increasing carbon fixation rates to make up for the loss flux. Despite there being no difference in *T. pseudonana* growth rates in either of our experiments, VOCs cannot be considered 'costless public goods' (Pacheco *et al*., 2019) because of the energetic costs associated with increasing carbon fixation to maintain *T. pseudonana* growth and homeostasis. Such cryptic physiological responses are challenging to measure but important for understanding the causes of variability in photosynthesis, which remain a major source of error in estimates of global primary production (Cullen, 1990; Behrenfeld and Falkowski, 1997).

Elevated carbon fixation was observed in another diatom, *Phaeodactulum tricornutum*. In that study, it was hypothesized that catabolism of diatom-derived carbon by attached bacterial communities alleviated CO_2 limitation at the diatom cell surface, thus stimulating carbon fixation (Samo *et al*., 2018). However, enhanced carbon fixation was heterogeneous in single-cell measurements and was only observed in one of two *P. tricornutum* co-

cultures examined (Samo *et al*., 2018). In another study, increased expression of transcripts associated with photosystem I and chlorophyll synthesis occurred in *Prochlorococcus* when growing in a co-culture with *Alteromonas* (Biller *et al*., 2016). Such changes may indicate that carbon fixation increased in *Prochlorococcus* in response to the heterotrophic consumption of carbon released by the algae, but carbon fixation was not directly measured (Biller *et al*., 2016).

We offer a similar explanation for observed increases in photosynthesis when phytoplankton are co-cultured with heterotrophs. The evidence we provide supports a mechanism in which bacterial metabolism of VOCs lowers VOC concentrations in the environment, causing an increase in the leakage of VOC metabolites from phytoplankton cells. This scenario assumes that the VOC metabolites in question are not end-products that have no further metabolic purpose and would be wasted. Increasing the flux of such compounds from cells would force phytoplankton to increase carbon fixation to maintain their growth rate. If this interpretation is correct, then bacterial catabolism of diffusible public goods couples VOC production and consumption in a VOC cycle that has a feedback mechanism, inducing more photosynthetic production and decreasing the efficiency of CO_2 conversion into phytoplankton biomass.

Our study, which used representatives of two of the most abundant microorganisms in the oceans, indicated VOC fluxes that we estimate are about 20% of carbon fixation. Rising awareness of VOC cycling has led to speculation about their contribution to the overall carbon cycle of the oceans. Across the entire ocean, gross primary production is estimated at 1.55×10^{17} g C year^{-1} (Marra, 2002; Westberry *et al*., 2008). If 20% of carbon fixed in the ocean is released from algae as VOCs, the total marine VOC production rate would be 3.10×10^{16} g C year^{-1}. This estimate is subject to large uncertainties, and likely depends on many unexplored factors, including growth conditions and community composition, but it establishes an approximate magnitude for the process we observed. Unexpectedly large fluxes of VOCs from phytoplankton and specialization in the oxidation of labile low-molecular-weight compounds, including VOCs, by SAR11 may partially explain how small, simple SAR11 cells capture an estimated 6%–37% of gross primary production (White *et al*., 2019).

Our results suggest that the VOC cycle can be a very significant component of carbon transfer from phytoplankton to bacteria. Further exploration of this topic likely will take varied paths, which might include further studies with cultured cells to define the metabolic origins, turnover times and fates of the wide variety of VOCs that are being detected in phytoplankton cultures. Also important will be field studies to measure these compounds in the environment, where, in many cases, they have seldom or never been reported. Defining the roles of VOCs will contribute to a better understanding of many features of the carbon cycle, for example, uncoupling of gross and net carbon fixation, the niches of heterotrophs, like SAR11, some of which paradoxically capture a large fraction of production with small genomes, and the variable influence of plankton on the atmosphere, where VOCs are engaged in complex chemistry.

Acknowledgements

The authors would like to thank Martin Schuster for use of the luminometer. This work was partially supported by the NASA North Atlantic Aerosols and Marine Ecosystems Study (NAAMES), award ID: NNX15AE70G, and the National Science Foundation, award ID: OCE-1436865.

References

Amin, S.A., Hmelo, L.R., van Tol, H.M., Durham, B.P., Carlson, L.T., Heal, K.R., *et al*. (2015) Interaction and signalling between a cosmopolitan phytoplankton and associated bacteria. *Nature* **522**: 98–101.

Barofsky, A., Vidoudez, C., and Pohnert, G. (2009) Metabolic profiling reveals growth stage variability in diatom exudates. *Limnol Oceanogr Method* **7**: 382–390.

Beale, R., Dixon, J.L., Arnold, S.R., Liss, P.S., and Nightingale, P.D. (2013) Methanol, acetaldehyde, and acetone in the surface waters of the Atlantic Ocean. *J Geophys Res Ocean* **118**: 5412–5425.

Becker, J.W., Hogle, S.L., Rosendo, K., and Chisholm, S.W. (2019) Co-culture and biogeography of *Prochlorococcus* and SAR11. *ISME J* **13**: 1506–1519.

Behrenfeld, M.J., and Falkowski, P.G. (1997) Photosynthetic rates derived from satellite-based chlorophyll concentration. *Limnol Oceanogr* **42**: 1–20.

Bidigare, R.R., Van Heukelem, L., and Trees, C. (2005) Analysis of algal pigments by high performance liquid chromatography. In *Algal Culturing Techniques*, Andersen, R. (ed). Burlington, MA: Elsevier Academic Press, pp. 327–345.

Biller, S.J., Coe, A., and Chisholm, S.W. (2016) Torn apart and reunited: Impact of a heterotroph on the transcriptome of *Prochlorococcus*. *ISME J* **10**: 2831–2843.

Bisutti, I., Hilke, I., and Raessler, M. (2004) Determination of total organic carbon – an overview of current methods. *TrAC Trends Anal Chem* **23**: 716–726.

Bjørrisen, P.K. (1988) Phytoplankton exudation of organic matter: why do healthy cells do it? *Limnol Oceanogr* **33**: 151–154.

Bromke, M.A., Giavalisco, P., Willmitzer, L., and Hesse, H. (2013) Metabolic analysis of adaptation to short-term changes in culture conditions of the marine diatom *Thalassiosira pseudonana*. *PLoS One* **8**: e67340.

Buchan, A., LeCleir, G.R., Gulvik, C.A., and González, J.M. (2014) Master recyclers: features and functions of bacteria associated with phytoplankton blooms. *Nat Rev Microbiol* **12**: 686–698.

Carini, P., Campbell, E.O., Morré, J., Sañudo-Wilhelmy, S. A., Thrash, J.C., Bennett, S.E., *et al*. (2014) Discovery of

a SAR11 growth requirement for thiamin's pyrimidine precursor and its distribution in the Sargasso Sea. *ISME J* **8**: 1727–1738.

Carini, P., Steindler, L., Beszteri, S., and Giovannoni, S.J. (2012) Nutrient requirements for growth of the extreme oligotroph '*Candidatus Pelagibacter ubique*' HTCC1062 on a defined medium. *ISME J* **7**: 592–602.

Colomb, A., Yassaa, N., Williams, J., Peeken, I., and Lochte, K. (2008) Screening volatile organic compounds (VOCs) emissions from five marine phytoplankton species by head space gas chromatography/mass spectrometry (HS-GC/MS). *J Environ Monit* **10**: 325–330.

Cotsaris, E., Bruchet, A., Mallevialle, J., and Bursill, D.B. (1995) The identification of odorous metabolites produced from algal monocultures. *Water Sci Technol* **31**: 251–258.

Cullen, J.J. (1990) On models of growth and photosynthesis in phytoplankton. *Deep Sea Res Part A Oceanogr Res Pap* **37**: 667–683.

Dachs, J., Calleja, M.L., Duarte, C.M., del Vento, S., Turpin, B., Polidori, A., *et al*. (2005) High atmosphere–ocean exchange of organic carbon in the NE subtropical Atlantic. *Geophys Res Lett* **32**: L21807.

Dani, K.G.S., and Loreto, F. (2017) Trade-off between dimethyl sulfide and isoprene emissions from marine phytoplankton. *Trends Plant Sci* **22**: 361–372.

Dixon, J.L., Beale, R., and Nightingale, P.D. (2013) Production of methanol, acetaldehyde, and acetone in the Atlantic Ocean. *Geophys Res Lett* **40**: 4700–4705.

Dixon, J.L., Beale, R., Sargeant, S.L., Tarran, G.A., and Nightingale, P.D. (2014) Microbial acetone oxidation in coastal seawater. *Front Microbiol* **5**: 1–9.

Facchini, M.C., Rinaldi, M., Decesari, S., Carbone, C., Finessi, E., Mircea, M., *et al*. (2008) Primary submicron marine aerosol dominated by insoluble organic colloids and aggregates. *Geophys Res Lett* **35**, L17814.

Fink, P. (2007) Ecological functions of volatile organic compounds in aquatic systems. *Mar Freshw Behav Physiol* **40**: 155–168.

Giovannoni, S., Halsey, K., Saw, J., Muslin, O., Suffridge, C., Sun, J., *et al*. (2019) A parasitic arsenic cycle that shuttles energy from phytoplankton to heterotrophic bacterioplankton. *mBio* **10**: e00246–e00219.

Giovannoni, S.J. (2017) SAR11 bacteria: the most abundant plankton in the oceans. *Ann Rev Mar Sci* **9**: 231–255.

Giovannoni, S.J., Tripp, H.J., Givan, S., Podar, M., Vergin, K.L., Baptista, D., *et al*. (2005) Genome streamlining in a cosmopolitan oceanic bacterium. *Science* **309**: 1242–1245.

Guillard, R.R.L., and Ryther, J.H. (1962) Studies of marine planktonic diatoms. I. Cyclotella nana Hustedt and *Detonula confervacea* Cleve. *Can J Microbiol* **8**: 229–239.

Halsey, K.H., Carter, A.E., and Giovannoni, S.J. (2012) Synergistic metabolism of a broad range of C1 compounds in the marine methylotrophic bacterium HTCC2181. *Environ Microbiol* **14**: 630–640.

Halsey, K.H., Giovannoni, S.J., Graus, M., Zhao, Y., Landry, Z., Thrash, J.C., *et al*. (2017) Biological cycling of volatile organic carbon by phytoplankton and bacterioplankton. *Limnol Oceanogr*, **62**, 2650–2661.

Hauser, E.J., Dickhut, R.M., Falconer, R., and Wozniak, A.S. (2013) Improved method for quantifying the air-sea flux of volatile and semi-volatile organic carbon. *Limnol Oceanogr Methods* **11**: 287–297.

Johnston, A., Crombie, A.T., El Khawand, M., Sims, L., Whited, G.M., McGenity, T.J., and Colin Murrell, J. (2017) Identification and characterisation of isoprene-degrading bacteria in an estuarine environment. *Environ Microbiol* **19**: 3526–3537.

Jüttner, F., Messina, P., Patalano, C., and Zupo, V. (2010) Odour compounds of the diatom *Cocconeis scutellum*: effects on benthic herbivores living on Posidonia oceanic. *Mar Ecol Prog Ser* **400**: 63–73.

Kolber, Z.S., Prášil, O., and Falkowski, P.G. (1998) Measurements of variable chlorophyll fluorescence using fast repetition rate techniques: defining methodology and experimental protocols. *Biochim Biophys Acta Bioenerg* **1367**: 88–106.

Landa, M., Burns, A.S., Roth, S.J., and Moran, M.A. (2017) Bacterial transcriptome remodeling during sequential co-culture with a marine dinoflagellate and diatom. *ISME J* **11**: 2677–2690.

Longnecker, K., Kido Soule, M.C., and Kujawinski, E.B. (2015) Dissolved organic matter produced by *Thalassiosira pseudonana*. *Mar Chem* **168**: 114–123.

Marra, J. (2002) Approaches to the measurement of plankton production. In *Phytoplankton Productivity*. Oxford, UK: Blackwell Science Ltd, pp. 78–108.

Mitchell, B.G., and Kieper, D.A. (1988) Variability in pigment particulate fluorescence and absorption spectra in the northeastern Pacific Ocean. *Deep Res* **35**: 665–689.

Myklestad, S.M. (2000) Dissolved organic carbon from phytoplankton. *Handb Environ Chem* **5**: 111–148.

O'Dowd, C.D., and de Leeuw, G. (2007) Marine aerosol production: a review of the current knowledge. *Philos Trans R Soc A* **365**: 1753–1774.

Pacheco, A.R., Moel, M., and Segrè, D. (2019) Costless metabolic secretions as drivers of interspecies interactions in microbial ecosystems. *Nat Commun* **10**: 103.

Paul, C., Mausz, M.A., and Pohnert, G. (2012) A co-culturing/metabolomics approach to investigate chemically mediated interactions of planktonic organisms reveals influence of bacteria on diatom metabolism. *Metabolomics* **9**: 349–359.

Paul, C., and Pohnert, G. (2011) Production and role of volatile halogenated compounds from marine algae. *Nat Prod Rep* **28**: 186–195.

Ritchie, R.J. (2006) Consistent sets of spectrophotometric chlorophyll equations for acetone, methanol and ethanol solvents. *Photosynth Res* **89**: 27–41.

Ruiz-Halpern, S., Sejr, M.K., Duarte, C.M., Krause-Jensen, D., Dalsgaard, T., Dachs, J., and Rysgaard, S. (2010) Air–water exchange and vertical profiles of organic carbon in a subarctic fjord. *Limnol Oceanogr* **55**: 1733–1740.

Samo, T.J., Kimbrel, J.A., Nilson, D.J., Pett-Ridge, J., Weber, P.K., and Mayali, X. (2018) Attachment between heterotrophic bacteria and microalgae influences symbiotic microscale interactions. *Environ Microbiol* **20**: 4385–4400.

Sargeant, S.L., Murrell, J.C., Nightingale, P.D., and Dixon, J. L. (2018) Basin-scale variability of microbial methanol uptake in the Atlantic Ocean. *Biogeosciences* **15**: 5155–5167.

Schmidt, R., Cordovez, V., De Boer, W., Raaijmakers, J., and Garbeva, P. (2015) Volatile affairs in microbial interactions. *ISME J* **9**: 2329–2335.

Shaw, S.L., Chisholm, S.W., and Prinn, R.G. (2003) Isoprene production by *Prochlorococcus*, a marine cyanobacterium, and other phytoplankton. *Mar Chem* **80**: 227–245.

Sinha, V., Williams, J., Meyerhöfer, M., Riebesell, U., Paulino, A.I., and Larsen, A. (2007) Air–sea fluxes of methanol, acetone, acetaldehyde, isoprene and DMS from a Norwegian fjord following a phytoplankton bloom in a mesocosm experiment. *Limnol Oceanogr* **55**: 1733–1740.

Spracklen, D.V., Arnold, S.R., Sciare, J., Carslaw, K.S., and Pio, C. (2008) Globally significant oceanic source of organic carbon aerosol. *Geophys Res Lett* **35**: L12811.

Srikanta Dani, K.G., Silva Benavides, A.M., Michelozzi, M., Peluso, G., Torzillo, G., and Loreto, F. (2017) Relationship between isoprene emission and photosynthesis in diatoms, and its implications for global marine isoprene estimates. *Mar Chem* **189**: 17–24.

Sun, J., Steindler, L., Thrash, J.C., Halsey, K.H., Smith, D. P., Carter, A.E., *et al*. (2011) One carbon metabolism in SAR11 pelagic marine bacteria. *PLoS One* **6**: e23973.

Sun, J., Todd, J.D., Thrash, J.C., Qian, Y., Qian, M.C., Temperton, B., *et al*. (2016) The abundant marine bacterium *Pelagibacter* simultaneously catabolizes dimethylsulfoniopropionate to the gases dimethyl sulfide and methanethiol. *Nat Microbiol* **1**: 16065.

Thornton, D.C.O. (2014) Dissolved organic matter (DOM) release by phytoplankton in the contemporary and future ocean. *Eur J Phycol* **49**: 20–46.

Tripp, H.J., Kitner, J.B., Schwalbach, M.S., Dacey, J.W.H., Wilhelm, L.J., and Giovannoni, S.J. (2008) SAR11 marine bacteria require exogenous reduced sulphur for growth. *Nature* **452**: 741–744.

Uitz, J., Claustre, H., Gentili, B., and Stramski, D. (2010) Phytoplankton class-specific primary production in the world's oceans: seasonal and interannual variability from satellite observations. *Global Biogeochem Cycles* **24**: GB3016.

Van Tol, H.M., Amin, S.A., and Armbrust, V. (2016) Ubiquitous marine bacterium inhibits diatom cell division. *ISME J* **11**: 31–42.

Weigert, M., and Kümmerli, R. (2017) The physical boundaries of public goods cooperation between surface-attached bacterial cells. *Proc R Soc B* **284**: 20170631.

Westberry, T., Behrenfeld, M.J., Siegel, D.A., and Boss, E. (2008) Carbon-based primary productivity modeling with vertically resolved photoacclimation. *Global Biogeochem Cycles* **22**: GB2024.

White, A., Giovannoni, S., Zhao, Y., Vergin, K., and Carlson, C. (2019) Elemental content and stoichiometry of SAR11 chemoheterotrophic marine bacteria. *Limnology and Oceanography Letters* **4**: 44–51.

Wright, S.W., Jeffrey, S.W., Mantoura, R.F.C., Llewellyn, C. A., Bjørnland, T., Repeta, D., and Welschmeyer, N. (1991) Improved HPLC method for the analysis of chlorophylls and carotenoids from marine phytoplankton. *Mar Ecol Prog Ser* **77**: 183–196.